

# Synthesis of Organic Compounds from Mixtures of Methane with Carbon Dioxide in Dielectric-Barrier Discharges at Atmospheric Pressure<sup>1</sup>

K. V. Kozlov,<sup>2</sup> P. Michel,<sup>3</sup> and H.-E. Wagner<sup>3,4</sup>

Received October 18, 2000; accepted February 12, 2001

---

The entire range of gas phase reaction products, depending on the composition of initial binary mixtures of methane and carbon dioxide in dielectric barrier discharges, has been determined (saturated as well as unsaturated hydrocarbons and oxygenated organic compounds). The macro-kinetics of the basic chemical pathways of the system under consideration has been investigated. This system is found to display a strong feedback effect (positive or negative, depending on the initial state of the surfaces, as well as the chemical composition of the feed-gas mixture). It is demonstrated that these properties undergo significant changes during operation, due to surface modification processes (polymer film deposition, its oxidation or reduction). They are found to exert a considerable influence on the chemical efficiency of the discharge (for example, on the absolute and relative chemical yields of the reaction products), the Lissajous figures appear to be a sensitive tool to monitor the operation conditions of the discharge.

---

**KEY WORDS:** Plasma chemistry; greenhouse gases; polymer films; dielectric-barrier discharge; organic synthesis.

## 1. INTRODUCTION

The first attempts at plasma-chemical conversion of the simplest gaseous compounds of carbon (CO, CO<sub>2</sub>, CH<sub>4</sub>) into more complex organic molecules date back to the 2nd half of the 19th century.<sup>(1–3)</sup> Much effort has since been devoted

<sup>1</sup>Article based on material presented at the 7<sup>th</sup> International Symposium on High Pressure, Low Temperature Plasma Chemistry—"Hakone VII"—held in Greifswald, Germany, September 10–13, 2000.

<sup>2</sup>Moscow State University, Department of Chemistry, 119899 Moscow, Russia.

<sup>3</sup>Institute of Physics, Ernst-Moritz-Arndt University of Greifswald, 17489 Greifswald, Domstrasse 10a, Germany.

<sup>4</sup>To whom all correspondence should be addressed. e-mail: wagner@physik.uni-greifswald.de

to find a suitable type of gas discharge system and optimal experimental conditions for the direct, efficient syntheses of certain valuable chemical products (eg., ethylene and acetylene,<sup>(4)</sup> formaldehyde and methanol,<sup>(5,6)</sup> formic acid,<sup>(7)</sup> etc.). Recently, a noticeable growth in interest towards this problem has followed the proposal to use a particular plasma-chemical technology, namely, dielectric barrier discharges (DBD), for the conversion of greenhouse gases (methane and carbon dioxide).<sup>(8)</sup> However, as yet no one commercially viable process of this type has been demonstrated. Two main drawbacks of plasma chemical technologies account for this state of affairs, namely, high energy consumption and low selectivity of the target products. Any further improvement of these process characteristics (hence, an increase in its efficiency) nowadays seem unlikely by way of empirical search methods for the optimal experimental conditions.

An alternative approach to this problem implies deep understanding of the basic physical and chemical processes, and development of an adequate theoretical model, which provides quantitative description for the system under consideration. Only then may it become possible to choose the most effective chemical pathway toward the desired product, to distinguish the limiting elementary steps, and to try to promote (or replace) them. Within the framework of such a general strategy, we have undertaken an experimental study of the chemical behaviour of  $\text{CO}_2 + \text{CH}_4$  mixtures in the DBD, focusing on a systematic analysis of the entire spectrum of reaction products. The choice in favor of the DBD has been made taking into account its unique physical properties (in particular, the highest value of the mean electron energy, compared to other types of electrical discharges), as well as a broad base of experience in its industrial application for ozone production.<sup>(9,10)</sup>

Apart from gas phase synthesis, the system under consideration may also be considered as a convenient plasma-chemical reactor for the production of polymer films. Already, preliminary experiments have demonstrated that such films can readily be formed on the electrode surfaces. Moreover, their appearance have been found to strongly influence the physical properties of the DBD, as well as the overall chemical efficiency of the reactor.<sup>(11–13)</sup>

The aim of the present study was to identify the dominant chemical pathways of organic compound formation from  $\text{CO}_2 + \text{CH}_4$  mixtures in a DBD reactor, and to investigate how certain electrical properties of the discharge influence chemical mechanisms and kinetics of this process, the gas mixture ratio being selected as the main experimental parameter. To characterize electrical properties of the DBD, the Lissajous figures technique has been used.<sup>(8,10–12)</sup> Quantitative chemical analysis of reaction products was performed by means of the highly sensitive gas chromatography—mass spectroscopy (GC-MS) method. In order to simplify the final kinetic analysis of the results, we have regulated the DBD power so as to provide very low conversion of the reagents, keeping the concentrations of reaction products in a ppm-range.

## 2. DESCRIPTION OF THE EXPERIMENT

### 2.1. Experimental Setup and Procedure

For our measurements, a closed system with gas flow circulation was used (Fig. 1a). To remove from the gas phase as many reaction products as possible and to collect them for the consequent analysis, a cold trap ( $T = -79^{\circ}\text{C}$ ) was installed on line after the DBD reactor. Before each experiment, the entire system was evacuated (to 0.5 mbar), filled with pure methane, and evacuated once again. Then, a gas mixture with the desired mixture ratio was prepared. Discharge treatment of this mixture was carried out under conditions of steady-state flow at a pressure of 1030–1050 mbar (that is slightly higher than outside the system), the temperature of the reactor being  $T = +90^{\circ}\text{C}$ . The duration of an experiment (treatment time) was chosen to be 20 min. Afterwards, that part of the gas system which included the cold trap was isolated and heated to  $T = +120^{\circ}\text{C}$ , and the quantitative chemical analysis of the gas samples from this closed volume was performed by means of the capillary gas chromatographic/mass spectrometric technique (using a SHIMADZU QP 5000 instrument).

It should be mentioned that the use of the cold trap (where reaction products are trapped and concentrated) may lead to certain artefacts due to some chemical reactions probably occurring in this concentrate (for example, an interaction between an alcohol and an acid to form the corresponding ester). Such possibility has been taken into account in the final kinetic analysis of experimental results.

The DBD reactor design was a classical parallel-plane electrode arrangement of the «metal - glass» type (Fig. 1b). To prevent a surface discharge from spreading to the upper surface of the dielectric (which would lead to undesirable distortion of the Lissajous figures, and to nonlinearity of the charge-voltage characteristics), the copper foil was covered with another glass plate of dimensions 60 mm  $\times$  70 mm  $\times$  5 mm (not shown in the figure), and the gap between two glass plates along the foil perimeter was carefully filled with epoxy resin. This precaution enabled us to obtain linearity of the main electrical parameters of the DBD (for example, transferred charge and electric power) over a wide range of amplitudes of the applied voltage.<sup>(11)</sup>

The standard electric circuit for charge-voltage measurements detected with an oscilloscope was employed using the test capacitance  $C_M = 10$  nF (Fig. 1c). The applied voltage of 9 kV amplitude and 50 Hz frequency provided a power input of about 650 mW. The total volume of the closed system being 5120 cm<sup>3</sup>, the latter value corresponds to a specific energy input of 0.15 J/cm<sup>3</sup> over the 20 min. duration of the experiment.

In order to compensate any possible influence of the gas mixture composition on the discharge burning voltage (consequently, upon the power input to the

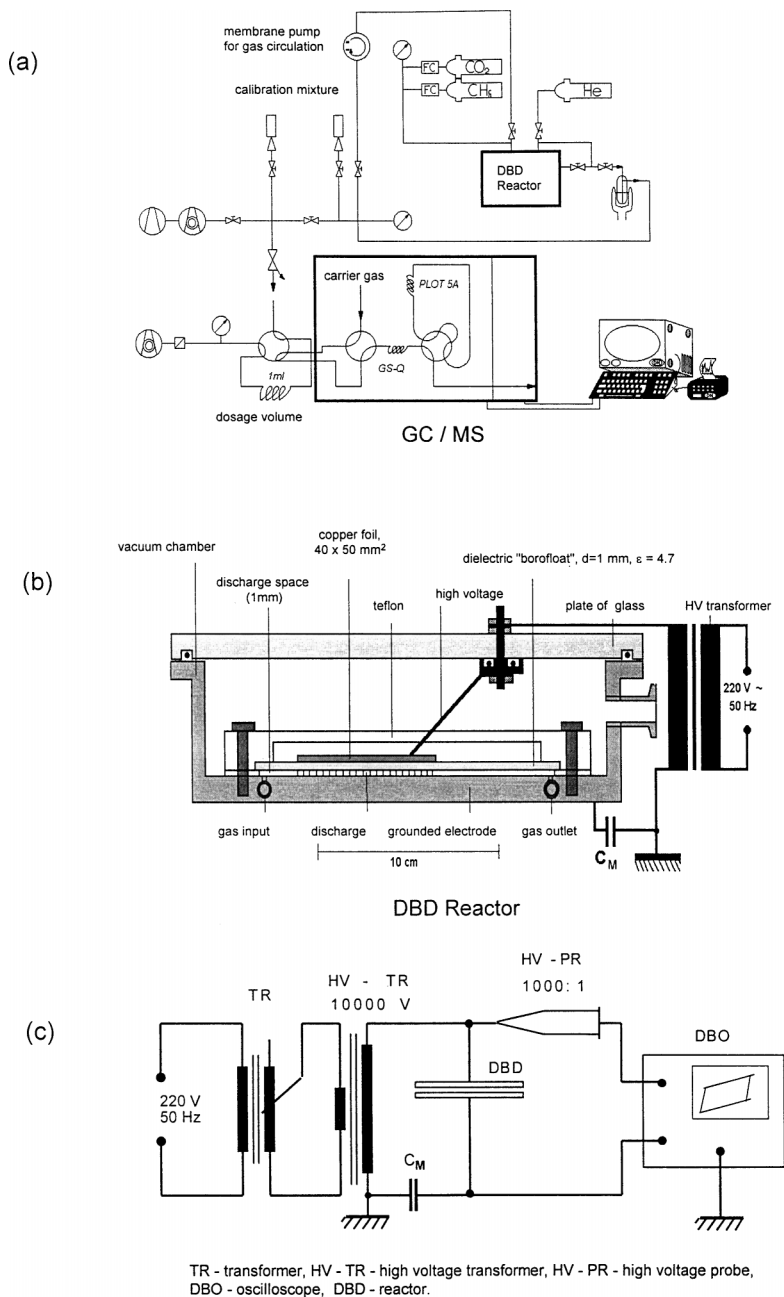


**Fig. 1.** (a) Experimental set-up; (b) discharge cell arrangement; (c) and a diagram of the electric circuit.

DBD), the applied voltage amplitude was always adjusted in such a way as to keep electrical power of the discharge constant for all experiments. It should be noted, however, that contrary to the case of binary  $\text{CH}_4 + \text{He}$  mixtures,<sup>(11)</sup> the burning voltage of the DBD in  $\text{CH}_4 + \text{CO}_2$  mixtures was found to depend little upon the mixture ratio, increasing monotonically from 2.9 kV for pure methane to 3.2 kV for pure  $\text{CO}_2$ .

## 2.2. Identification and Quantitative Analyses of Reaction Products

Identification of individual chemical compounds in the reaction product mixtures was carried out by comparing a mass-spectrum corresponding to each of the observed chromatographic peaks with the spectra presented in the standard library of the GC-MS instrument. The results of this procedure are summarized in the Tables I and II. For the saturated  $\text{C}_1$ — $\text{C}_4$  hydrocarbons (including Isobutane), formaldehyde and methanol, the correctness of their identification was confirmed by direct calibration with these pure compounds. Although all the peaks of experimental chromatograms (even the least intense) have been identified, some uncertainties persisted for certain compounds produced in very low concentrations

**Table I.** List of Hydrocarbons Detected in the Mixture of Reaction Products

Compound	Brief formula	Mass value used	Measured
Structural formula	Name	used in the text of this paper	for the CG-peak calibration
			concentration, ppm
Saturated hydrocarbons			
$\text{CH}_3\text{—CH}_3$	ethane	$\text{C}_2\text{H}_6$	26
$\text{CH}_3\text{—CH}_2\text{—CH}_3$	propane	$\text{C}_3\text{H}_8$	39
$\text{CH}_3\text{—CH}_2\text{—CH}_2\text{—CH}_3$	n-butane	$\text{n-C}_4\text{H}_{10}$	43
$\begin{array}{c} \text{CH}_3 \\   \\ \text{CH}_3\text{—CH—CH}_3 \end{array}$	isobutane	$\text{i-C}_4\text{H}_{10}$	43
$\text{CH}_3\text{—CH}_2\text{—CH}_2\text{—CH}_2\text{—CH}_3$	n-pentane	$\text{n-C}_5\text{H}_{12}$	43
Unsaturated hydrocarbons			
$\text{CH}_2\text{=CH}_2$	ethylene	$\text{C}_2\text{H}_4$	26
$\text{CH}\equiv\text{CH}$	acetylene	$\text{C}_2\text{H}_2$	26
$\text{CH}_2\text{=CH—CH}_3$	propylene	$\text{C}_3\text{H}_6$	39
$\text{CH}_2\text{=C=CH}_2$	1,2-propadiene	$\text{s-C}_3\text{H}_4$	39
$\text{CH}\equiv\text{C—CH}_3$	1-propyne	$\text{a-C}_3\text{H}_4$	39
$\text{CH}_2\text{=CH—CH}_2\text{—CH}_3$	1-butene	$\text{a-C}_4\text{H}_8$	41
$\text{CH}_3\text{—CH=CH—CH}_3$	2-butene	$\text{s-C}_4\text{H}_8$	41
$\text{CH}\equiv\text{C—CH}_2\text{—CH}_3$	1-butyne	—	50
$\text{CH}_2\text{=CH—C}\equiv\text{CH}$	1-buten-3-yne	—	50
$\text{CH}\equiv\text{C—C}\equiv\text{CH}$	1,3-butadiyne	$\text{C}_4\text{H}_2$	50
$\text{CH}_2\text{=CH—CH}_2\text{—CH}_2\text{—CH}_3$	1-pentene	—	55

<sup>a</sup>After 20 minutes of treating of pure methane in the DBD at atmospheric pressure.

**Table II.** List of Oxygenated Organic Compounds Detected in the Mixtures of Methane with Carbon Dioxide after Their Treatment in the DBD

Compound		Brief formula or abbreviation of the name used in the text of this paper	Mass value used for the CG-peak calibration	Maximum of the measured concentration, ppm
Structural formula	Name			
$\text{H}_2\text{C}=\text{O}$	formaldehyde	$\text{H}_2\text{CO}$	30	2.7
$\text{CH}_3-\text{OH}$	methanol	$\text{CH}_3\text{OH}$	29	0.8
	ethylene oxide	ETO	29	15
$\text{H}_2\text{C}-\text{CH}_2$				
$\text{CH}_3-\text{O}-\text{CH}_3$	dimethyl ether	DME	46	0.3
$\text{CH}_3-\text{O}-\text{CH}=\text{O}$	methyl formate	MF	60	0.2
	propylene oxide	PO	58	0.3
$\text{H}_2\text{C}-\text{CH}-\text{CH}_3$				
	acetone	Ac.	43	1
$\text{CH}_3-\text{C}-\text{CH}_3$				

(namely, some unsaturated  $\text{C}_4$  and  $\text{C}_5$  hydrocarbons). For these species, it was impossible to obtain the entire mass-spectrum, since their concentration was near the lower sensitivity limit of the instrument.

Most of the gas mixtures subjected to chromatographic analyses also contained five compounds which are not listed in Tables I and II, namely  $\text{CH}_4$ ,  $\text{CO}_2$ ,  $\text{CO}$ ,  $\text{H}_2$  and  $\text{H}_2\text{O}$ . Two peaks corresponding to  $\text{CH}_4$  and  $\text{CO}_2$ , with rare exceptions, were the dominant ones in the chromatogram, but they were never used for quantitative analyses, for the following reason. Under these-described experimental conditions the extent of conversion of the reagents ( $\text{CH}_4$  and  $\text{CO}_2$ ) was so low that their concentrations did not change appreciably during plasma treatment, the absolute values of these concentrations being initially defined by the gas mixture ratio. Furthermore, quantitative determination of  $\text{CO}$ ,  $\text{H}_2$  and  $\text{H}_2\text{O}$  was not possible by the chromatographic analysis procedure we had selected. But since we are interested mostly in plasma-chemical synthesis of organic compounds, we made no particular efforts to overcome these limitations of our methodology.

Although they are not monitored within the present experimental study, the latter three gases are well-known to be produced under the present DBD conditions. Moreover, the formation of the so-called synthesis gas via the overall reaction  $\text{CH}_4 + \text{CO}_2 \rightarrow 2\text{H}_2 + 2\text{CO}$  has been shown to be a dominant reaction channel over a wide range of the gas mixture ratio variation.<sup>(14,15)</sup> Molecular hydrogen is obviously formed in mixtures enriched with methane, as a by-product of the synthesis of saturated and unsaturated hydrocarbons. In the case of mixtures enriched with carbon dioxide, hydrogen is likely oxidized to form water.

The quantitative GC-MS analyses of reaction products were carried out by measuring the heights of chromatographic peaks corresponding to the preliminary

selected values of molecular masses for every individual component of the mixture (GC partial peaks). This selection procedure was designed to maximize the sensitivity of the previously-described experimental method (in particular, to avoid overlapping of neighboring partial GC peaks of different chemical compounds). Thus, chosen values of molecular masses are shown listed in Tables I and II. For the saturated C<sub>1</sub>—C<sub>4</sub> hydrocarbons (including Isobutane), formaldehyde and methanol, the values of their concentrations were determined from the heights of the corresponding partial GC peaks using direct calibration. Concentrations of other reaction products were estimated by assuming that the calibration curves for organic compounds of the same chemical type and similar molecular mass behave similarly. So, the calibration data for C<sub>2</sub>H<sub>6</sub> were used also for C<sub>2</sub>H<sub>4</sub> and C<sub>2</sub>H<sub>2</sub>, and those for C<sub>3</sub>H<sub>8</sub> and n-C<sub>4</sub>H<sub>10</sub> were applied, respectively, to all the other C<sub>3</sub> and C<sub>4</sub> compounds (with the exception of Isobutane). The calibration curve for methanol (CH<sub>3</sub>OH) was used also for dimethyl ether (DME) and ethylene oxide (ETO), and that for formaldehyde (H<sub>2</sub>CO) was applied to methyl formate (MF), propylene oxide (PO) and acetone (Ac). In order to compensate possible errors resulting from the use of the different partial peaks for the compounds with different mass spectra, the heights of the selected partial peaks were recalculated taking into account their sensitivity factors and intensity distributions over a spectrum; the data required for this came from the standard library of the GC-MS instrument.

Thus, in the latter case, the accuracy in determining absolute values of the species concentrations is only order-of-magnitude, however, the relative accuracy (which is important for comparing the measured results of the same reaction products in different experiments) is comparable to that of compounds which were calibrated directly. The sensitivity of GC-MS analysis under the present conditions (and taking into account background noise) is estimated at about 0.1 ppm for hydrocarbons, and about 0.05 ppm for oxygenated organic compounds.

### 2.3. Recovery of the DBD Reactor Chemical Efficiency

Already the preliminary experiments had shown that CO<sub>2</sub> + CH<sub>4</sub> feed gas mixtures with more than 3–5%, of CO<sub>2</sub>, the results of the GC-MS analyses appeared to be irreproducible<sup>(12)</sup> That is, every repetition of an experiment under the same conditions resulted in a considerable decrease (about 20–30%) in the yields of almost all the reaction products, despite thorough cleaning of the discharge chamber and evacuation of the entire system before preparing the working gas mixture. To analyze this phenomenon we supposed, first, that chemical efficiency of the DBD is highly sensitive to the properties of the glass surface, and second, that these properties change with plasma-exposure of the electrode (possibly, due to deposition of polymer-like films and subsequent plasma-chemical oxidation or reduction of the films<sup>(13,16,17)</sup>). The following experimental findings confirmed

these hypotheses:

1. For any chosen gas mixture, the highest yields of reaction products were obtained when a new, clean glass plate was installed in the discharge cell.
2. For pure methane, the yields of hydrocarbons were found to decrease monotonically during the first 30–40 min. after installation of a fresh glass plate. Then a steady-state was reached, corresponding to 70–80% of the highest initial product yield values, similar to what had been observed earlier.<sup>(16)</sup>
3. Chemical oxidation of the “contaminated” glass electrode surface (that is coated with a polymer-like film by earlier exposure to DBD in methane, described earlier) results in a drastic reduction in the product yields (by more than an order of magnitude). The oxidation was carried out with standard reagents (an aqueous solution of  $\text{KMnO}_4$  with  $\text{H}_2\text{SO}_4$ ), following which the glass plate was thoroughly rinsed in distilled water and dried. A similar decrease in the DBD efficiency was observed after a 20 min. plasma treatment of the “contaminated” glass electrode in pure  $\text{CO}_2$ .
4. Plasma-chemical reduction of the initially oxidized electrode surface in hydrogen or in methane led to noticeable improvement in chemical efficiency of the DBD reactor.

By using the latter experimental finding, we managed to stabilize the DBD properties, thus providing reproducible initial conditions, at least at the beginning

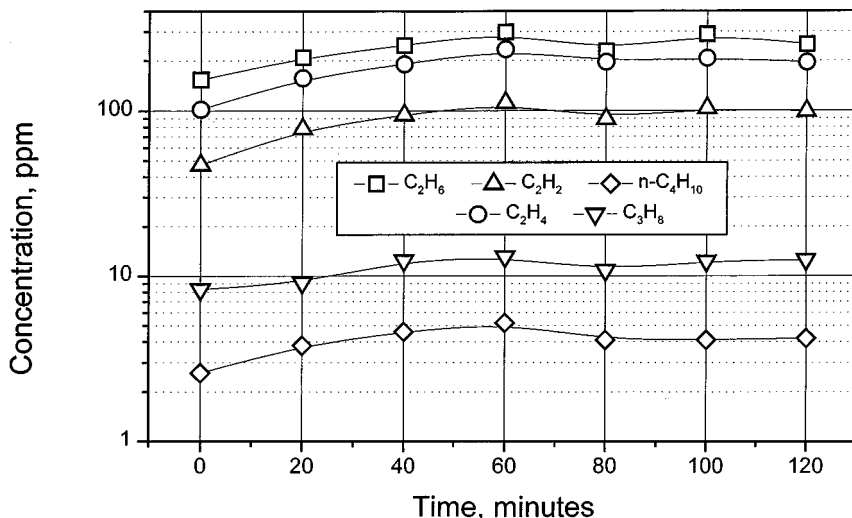


**Fig. 2.** Typical example for the DBD chemical efficiency stabilization carried out by means of the plasma treatment (by the discharge itself in pure methane) of initially oxidized electrode surface. See explanations in the text.

of each experiment. The stabilization procedure consisted of a sequence of standard experiments in pure methane, the quality of the dielectric surface being monitored by measuring reaction product concentrations (see Fig. 2). This procedure preceded all other experiments, presented in the following.

### 3. RESULTS AND DISCUSSION

#### 3.1. Formation of Hydrocarbons

Chemical compositions of the mixtures of hydrocarbons synthesized in the DBD reactor from  $\text{CO}_2 + \text{CH}_4$ ,  $\text{CH}_4 + \text{He}$ , and  $\text{CO}_2 + \text{CH}_4 + \text{He}$  were found to be qualitatively similar to that for pure methane (Table I). For the  $\text{C}_2$ — $\text{C}_4$  compounds, almost all of the possible chemical isomers were identified as reaction products, except the cyclic ones (cyclopropane, cyclobutane). Only two representatives of the  $\text{C}_5$ -hydrocarbons (*n*-pentane and 1-pentene) were detected, and their concentrations were near the sensitivity limit of the instrument.

In our experiments, the highest chemical yields were always obtained for  $\text{C}_2\text{H}_6$ ,  $\text{C}_2\text{H}_4$  and  $\text{C}_2\text{H}_2$ , compared with other hydrocarbons. Contrary to most reaction products which were collected in the cold trap, these three compounds remained in the gas phase, since their boiling points are below  $-79^\circ\text{C}$ . Therefore, in the closed system with a gas flow circulation, they were subjected to plasma treatment in the DBD reactor from the moment of their formation until the end of experiment. This peculiarity of our experimental procedure accounts for the observed variety and relatively high yields of the  $\text{C}_3$ — $\text{C}_5$  hydrocarbons collected in the cold trap. Besides, it determines mainly the macro-kinetics of the  $\text{C}_2$ -hydrocarbon synthesis from the  $\text{CO}_2 + \text{CH}_4$  mixtures (Fig. 3).

The chemical mechanism for  $\text{C}_2$ -hydrocarbons formation in DBD from pure methane was originally established by St. Aune<sup>(18)</sup> and later confirmed by Zhitnev and Filippov.<sup>(16)</sup> It was experimentally proved that the process consists of the following three sequential steps:



Assuming validity of this mechanism also for  $\text{CO}_2 + \text{CH}_4$  mixtures and supposing  $\text{CO}_2$  to be chemically inert, we might expect the concentrations of  $\text{C}_2$ -hydrocarbons to be proportional to the content of  $\text{CH}_4$  in the feed gas. As it is clearly seen from Fig. 3, this is observed experimentally only for the  $\text{C}_2\text{H}_6$  concentration, and only in the central part of the  $\text{CH}_4$  concentration range. Two different deviations from proportionality can be distinguished here:

- (a) the appearance of local minima and maxima on the curves, corresponding to  $\text{CO}_2$  concentrations of about 1% and 3%, respectively;
- (b) in the cases of  $\text{C}_2\text{H}_4$  and  $\text{C}_2\text{H}_2$ , a greater than linear drop in the concentration curves, with rising  $\text{CO}_2$  content.

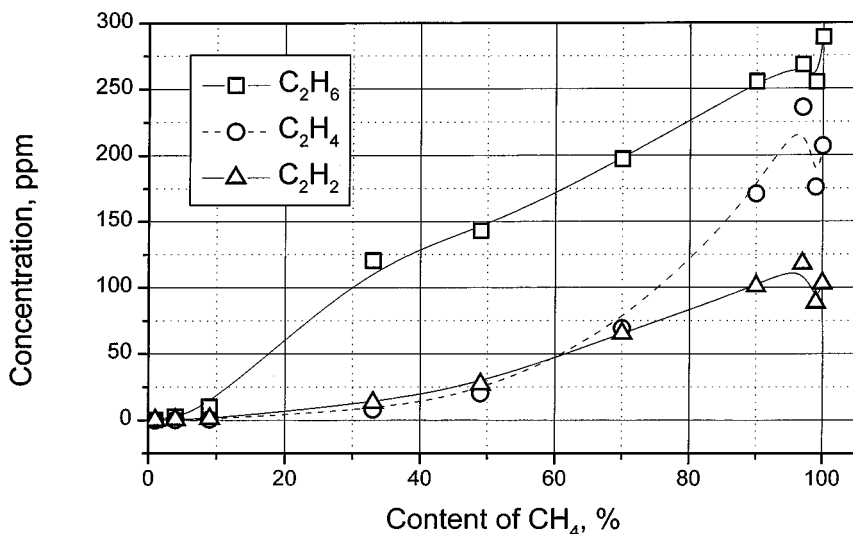
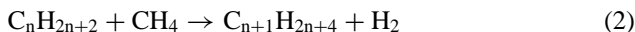


Fig. 3. Formation of C<sub>2</sub>-hydrocarbons from the mixtures of CH<sub>4</sub> with CO<sub>2</sub> in the DBD. The influence of the gas mixing ratio on the reaction product concentrations.

By repeating several times the experiments in mixtures with low CO<sub>2</sub> concentrations, we proved that the type (a) deviations cannot be attributed to the scatter of the data. To explain this behavior of the curves, it seems sufficient to assume that only the rate constant of the gross reaction  $\text{CH}_4 \rightarrow \text{C}_2\text{H}_6$  (that is initial step in the general scheme (1)) undergoes certain changes with increasing CO<sub>2</sub> concentration. These changes may be caused as by the influence of the feed gas mixture composition on the electron energy distribution function, as by the certain alterations of the DBD mechanism.<sup>(10,11)</sup> It should be noted that deviations of the type (a) were also observed for most of the hydrocarbons listed in Table I (see Fig. 4).

Deviations of type (b) may be attributed to chemical participation by CO<sub>2</sub> in scheme (1), that is, to the appearance of some additional reaction pathways which consume C<sub>2</sub>H<sub>4</sub> (probably, via oxidation and/or polymerization processes).

Comparing the concentrations of the five saturated hydrocarbons detected in the reaction products for CO<sub>2</sub> contents varying between 0 and 10% (Fig. 4) leads one to the following conclusion. In the two series of homologous compounds, namely, C<sub>2</sub>H<sub>6</sub>—C<sub>3</sub>H<sub>8</sub>—i-C<sub>4</sub>H<sub>10</sub> and n-C<sub>4</sub>H<sub>10</sub>—n-C<sub>5</sub>H<sub>12</sub>, the concentrations decrease approximately by a factor 20 with each unit increase in carbon chain length. Therefore, it seems reasonable to assume that a carbon chain growth occurs mainly via an overall reaction of the type



the only exception being the transition  $\text{C}_3\text{H}_8 \rightarrow \text{n-C}_4\text{H}_{10}$ . In the latter case the concentration of n-C<sub>4</sub>H<sub>10</sub> is half that of C<sub>3</sub>H<sub>8</sub>, that is, an order of magnitude

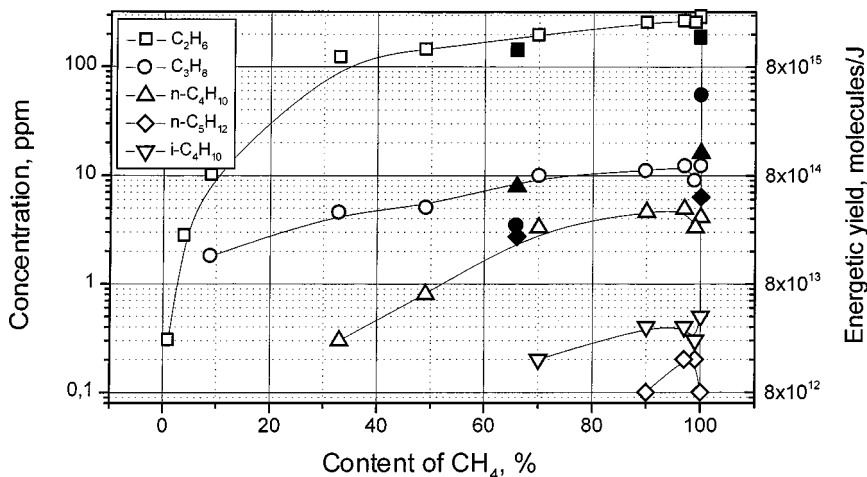


**Fig. 4.** Formation of saturated hydrocarbons ( $C_2$ – $C_5$ ) from the mixtures of  $CH_4$  with  $CO_2$  in the DBD. Comparison of the energetic yields of these compounds with the experimental results of Eliasson *et al.*<sup>(20)</sup> (black solid signs, right vertical axis).

higher than expected. This may be explained by the existence of an additional reaction pathway for  $n$ - $C_4H_{10}$  formation,<sup>(19)</sup> namely:



which appears to be more effective than the  $C_3H_8 + CH_4$  reaction under the present experimental conditions.

It is interesting to compare energetic yields of unsaturated hydrocarbons with the published experimental results of Eliasson *et al.*<sup>(20)</sup> (Fig. 4, black solid symbols), obtained in a DBD reactor with an open gas flow system, but for very high electrical power density (almost 3 orders of magnitude higher than in our experiments) at a frequency of 18 kHz. Despite the substantial differences in experimental conditions, the values of energetic yields for  $C_2H_6$  are quite comparable, at least within the 0–33% range of  $CO_2$  content, but the concentrations of other saturated hydrocarbons appear to be higher under experimental conditions used by Eliasson *et al.*<sup>(20)</sup> However for the case of pure  $CH_4$ , their measured ratios for successive members of the homologous series  $C_2H_6$ – $C_3H_8$ – $n$ - $C_4H_{10}$ – $n$ - $C_5H_{12}$  are seen to be roughly constant, without exception. Hence, for pure  $CH_4$ , the experimental data<sup>(20)</sup> also comply with the general kinetic scheme (2) but, contrary to our own results, the contribution of the overall reaction (3) may be neglected. The most likely reason for these differences seems to be that our closed gas flow system provides continuous plasma treatment to  $C_2H_6$  accumulated in the gas phase.

### 3.2. Synthesis of Oxygenated Organic Compounds

Taking into account the great variety of hydrocarbons detected in the reaction product mixture, the corresponding list of oxygenated organic compounds appears to be surprisingly short (compare Tables I and II): four derivatives of C<sub>1</sub>-compounds, including two ethers (DME and MF), only one representative of C<sub>2</sub>-derivatives (ETO), and two oxygenated compounds with 3 carbons (PO and Ac.). Besides, from the comparison of the data presented in the right columns of the Tables I and II, it is clearly seen that the concentrations of the oxygenated reaction products are considerably lower than those of the hydrocarbons, usually below 1 ppm, that is, just above the sensitivity limit of the detector. Therefore, it seems reasonable to assume that really several other oxygenated organic compounds are also formed (e.g., ethanol, acetaldehyde etc.), but in trace quantities (i.e., below 0.1 ppm) which cannot be detected by means of the GC-MS instrument used here.

Thus, the following important conclusion emerges from our experimental results, namely, that the chemical yields of hydrocarbons obtained from the CH<sub>4</sub> + CO<sub>2</sub> mixtures in the DBD are considerably higher than those of the oxygen-containing organic substances. Possible reasons for such a peculiarity of the general scheme for chemical pathways will be discussed under item 4 of this article.

The plots for experimentally-measured concentrations of all the oxygenated organic compounds listed in Table II versus mixture ratio are presented in Fig. 5.

For most CH<sub>4</sub> concentrations, ETO was found to be the dominant product among the oxygenated compounds (Fig. 5a). It was observed at the concentrations of about 1 ppm even in the case of pure CH<sub>4</sub>, but only in the experiments with the «recovered» electrode surface which had been initially treated by plasma in CO<sub>2</sub> containing gas mixtures. No traces of ETO and other oxygenated compounds were detected in the volume of experimental system after its evacuation and filling with methane, but before the discharge. Therefore, an appearance of ETO and some other species (see Fig. 5) in the reaction products may be considered as an additional evidence for the de-polymerization processes occurring in the DBD.

Even a simple, qualitative kinetic analysis of the results presented in Fig. 5 enables to distinguish the following general features of the process.

Except DME, the highest yields of the products are reached not in the center of the concentration scale (50% CH<sub>4</sub> + 50% CO<sub>2</sub>), but shifted either to the right (ETO, PO and Ac.), or to the left (MF, H<sub>2</sub>CO and CH<sub>3</sub>OH). Hence, the simplest one-step macro-kinetic scheme for the overall reaction of type CH<sub>4</sub> + CO<sub>2</sub> → *Products*, which obviously implies electron impact dissociation of the reagents (CH<sub>4</sub> + e → CH<sub>3</sub> + H + e, and CO<sub>2</sub> + e → CO + O + e) to be the limiting stage of the entire plasma-chemical process, can provide a valid macro-kinetic description only in the case of the DME synthesis.

Taking into account the existence of unsaturated hydrocarbons with double bonds in the reaction products, it seems quite reasonable to propose the following

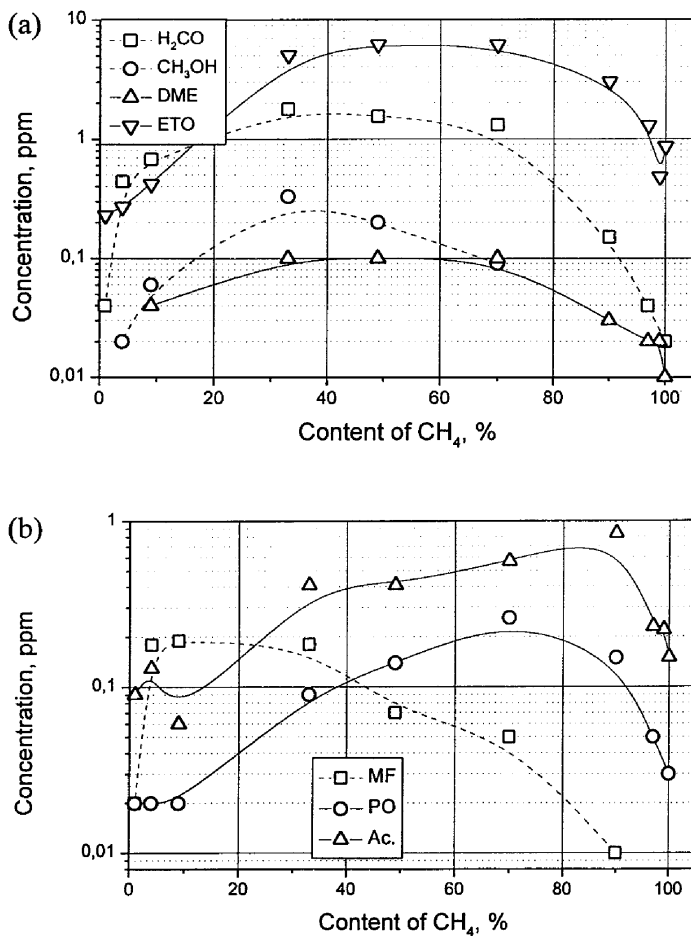


Fig. 5. Formation of oxygenated organic compounds from the mixtures of CH<sub>4</sub> with CO<sub>2</sub> in the DBD. The influence of the gas mixing ratio on the reaction product concentrations.

two overall reactions for the description of the ETO and PO formation macrokinetics:



Obviously, the scheme (4,5) provides at least a qualitative explanation for the shift of the corresponding concentration curve maxima towards the higher CH<sub>4</sub> content



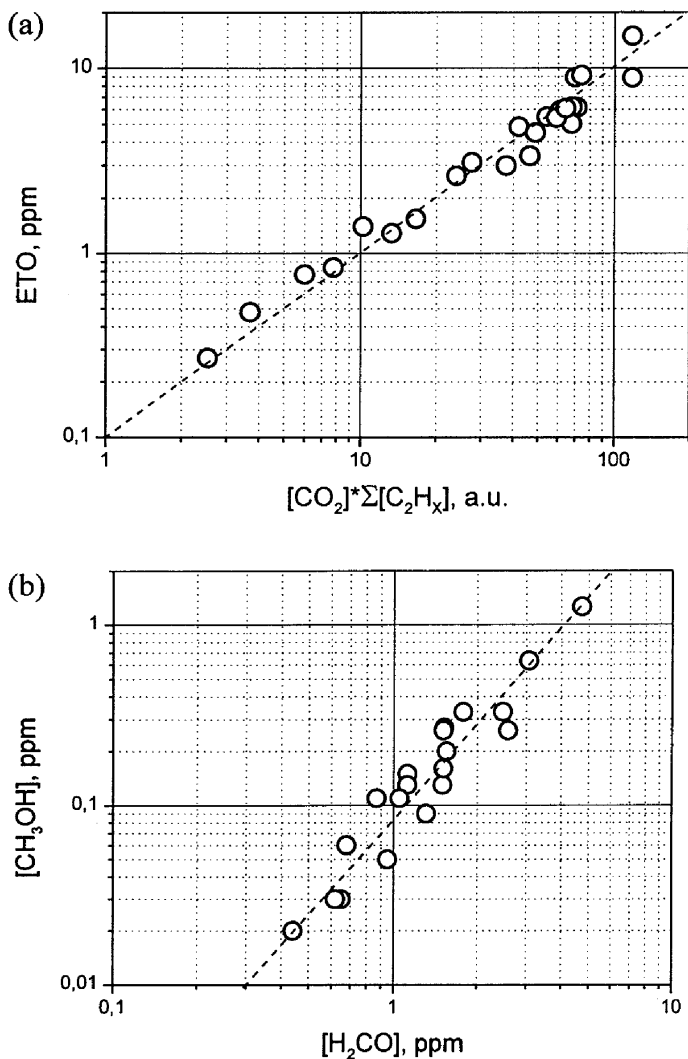


**Fig. 6.** Experimentally observed correlation. (a) between the concentration of ethylene oxide and the product  $[\text{CO}_2] \cdot \sum [\text{C}_2\text{H}_x]$ , the latter quantity being calculated for  $[\text{C}_2\text{H}_4]$  given in ppm, and for  $[\text{CO}_2]$  given in mole fractions; between the concentrations of formaldehyde and methanol.

1.8 with respect to formaldehyde for the hypothetical generalized reaction  $\text{H}_2\text{CO} + \text{other reagents} \rightarrow \text{CH}_3\text{OH} + \text{other products}$ . Obviously, this value of the rate order does not comply with the reaction scheme of the consequent hydrogenation of formaldehyde.<sup>(21)</sup> The simplest overall reaction which accounts for the

experimentally-observed correlation, at least qualitatively, seems to be



Besides the hypothetical reaction channel (7), there is another possible macrokinetic scheme which provides a reasonable explanation for the results presented in Fig. 6b. The latter scheme assumes two parallel chemical reactions for the formation of  $\text{H}_2\text{CO}$  and  $\text{CH}_3\text{OH}$  from the same intermediate compound (radical), occurring with different rate orders (i.e., 2 for methanol, and 1 for formaldehyde).

As regards the formation of MF, the following important remark should be made here. This substance may be synthesized not in the DBD reactor, but in the trap during heating, as a result of the usual ester formation process (via interaction between methanol and formic acid accumulated in the cold trap). Therefore, assuming formic acid to be one of the products of the plasma-chemical conversions in the mixtures  $\text{CH}_4 + \text{CO}_2$ , we may treat MF as its indicator. In our experiments, formic acid itself has never been detected in the gas phase product mixtures, probably because of its high boiling point ( $160^\circ\text{C}$ ).

### 3.3. Properties of the Dielectric Surface, Electrical Characteristics of the DBD and Its Chemical Efficiency

As already mentioned earlier, the chemical efficiency of the DBD in methane and its mixtures with carbon dioxide appears to be very sensitive to the state of the dielectric surface. To explain such a sensitivity, we assumed first, that the following surface modification processes can occur in the present system: polymer film deposition with its consequent plasma-chemical oxidation or reduction; and second, due to these processes, the microscopic electrical properties of the DBD (i.e., the properties of the individual microdischarges) undergo significant changes, thus influencing the overall chemical efficiency of the plasma treatment.<sup>(12,13)</sup> In our experiments, additional evidence for the existence of these polymer films has been obtained, namely, evidence for the depolymerization processes occurring in the discharge in pure He. These test experiments were carried out as follows. After a certain period (about 1 hour) of the DBD operation in pure  $\text{CH}_4$  (gas 1) or in the mixture 50%  $\text{CH}_4 + 50\%$   $\text{CO}_2$  (gas 2) the reactor chamber was evacuated, filled with He had then subjected to 20 min. plasma treatment. Afterwards, the GC-MS analysis of the working gas has shown the traces of  $\text{C}_2\text{H}_4$  and  $\text{C}_2\text{H}_2$  in the gas 1; and the traces of  $\text{C}_2\text{H}_4$ ,  $\text{C}_2\text{H}_2$ ,  $\text{H}_2\text{CO}$ , ETO, PO and Ac. in the gas 2. All these compounds may be treated as the products of plasma assisted depolymerization of a hydrocarbon polymer film, e.g., polyethylene (case of the gas 1), and of some oxygen-containing polymer film (case of the gas 2). Formation of oxygen-containing polymers under the similar conditions of corona discharges has been reported by Ruzinska *et al.*<sup>(17)</sup>

**Table III.** Experimental Conditions for the Results Presented in Figs. 7 and 8

A	Glass electrode after recovery (60 min. of plasma treatment in pure CH <sub>4</sub> ); feeding gas mixture: He (50%), CH <sub>4</sub> (25%), CO <sub>2</sub> (25%)
B	New glass electrode, feeding gas mixture: CH <sub>4</sub> (50%), CO <sub>2</sub> (50%)
C	Glass electrode after 60 min. of plasma treatment in the gas mixture: CH <sub>4</sub> (50%), CO <sub>2</sub> (50%); feeding gas mixture of the same composition
D	Glass electrode after recovery (60 min. of plasma treatment in pure CH <sub>4</sub> ); feeding gas mixture as for B,C
E	Glass electrode covered with ceramics (see text), feeding gas mixture as for B,C,D

In order to clarify the mechanism of the profound influence of the state of the dielectric electrode surface on the chemical efficiency of the DBD in the mixtures CH<sub>4</sub> + CO<sub>2</sub>, we performed a series of experiments, keeping constant the gas mixing ratio (1:1), and varying initial conditions referring to the dielectric electrode (Table III: B–D).

Two additional experimental arrangements (Table III: A,E) have been added to this series taking into account the following idea. There are two important characteristics of barrier discharge that can be affected by the properties of dielectric material: the mean effective value of electron energy, and the mean effective value of electric power density (specific power).<sup>(10)</sup> To model the effect of an increase of the mean electron energy, we used an addition of 50% He to our standard mixture (Table III: A). To increase the mean value of specific power, we covered the glass electrode with a thin plate of a ferroelectric ceramic ( $\epsilon = 6000$ ), keeping constant the discharge gap width and the total capacitance (Table III: E). It should be noted that here specific power is considered locally, i.e., it is related to the volume of the microdischarge channels, but not to the whole volume of the discharge gap. Using of ferroelectric ceramic as a dielectric barrier has proven to result in a considerable increase in current density and transferred charge within the discharge filaments.<sup>(10,22)</sup>

Under certain experimental conditions (namely, when the total discharge area is not much greater than the area of dielectric surface occupied by a single microdischarge<sup>(10)</sup>), the charge-voltage characteristics of a DBD (Lissajous figures) can reflect its internal structure, e.g., the magnitude of transferred charge for individual microdischarge or microdischarge series.<sup>(11)</sup> In this case a number of «steps» appears instead of a straight line on the right, left or on both sides of the common parallelogram (Fig. 7). The distance between the neighboring «steps» may be treated as a measure for transferred charge value.<sup>(10,11)</sup>

The charge-voltage characteristics of the DBD in methane-containing gas mixtures were found to be very sensitive as to the gas mixture ratio,<sup>(11)</sup> as to the kind (state of the surface) of the dielectric used (Fig. 7). This sensitivity accounts for the usually observed temporal alterations in the shape of the Lissajous figures, the latter taking place mostly during the first 3–5 min. of each experiment. Such a period of time was necessary for the system under consideration to reach steady-state

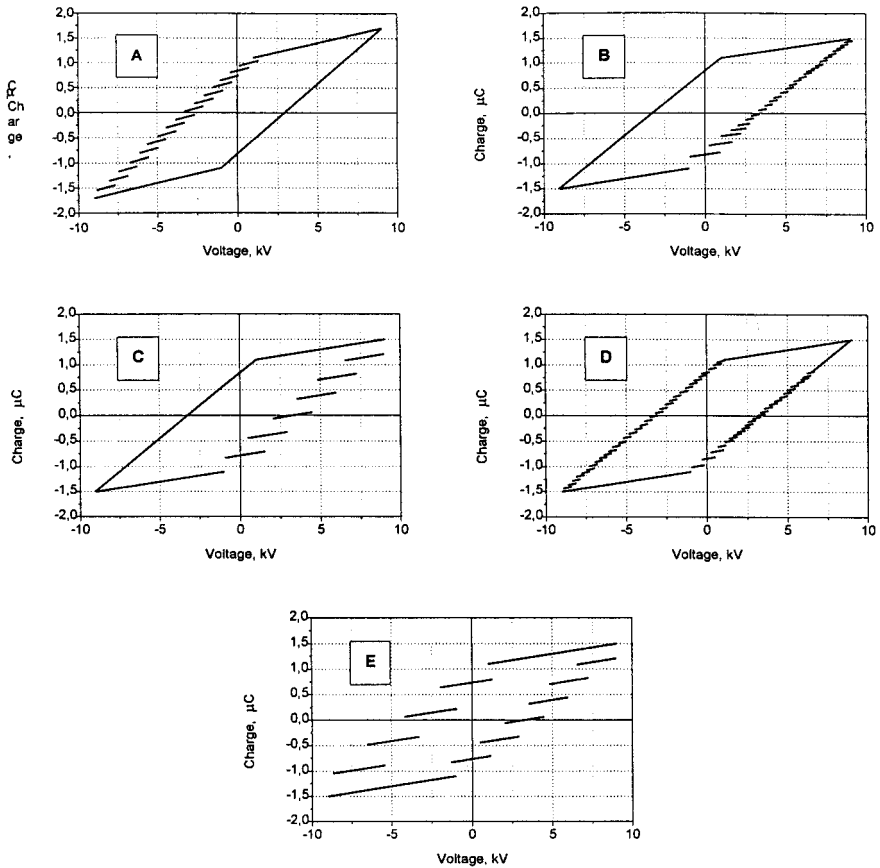


**Fig. 7.** Charge-voltage characteristics (Lissajous figures) of the DBD in the mixtures of  $\text{CH}_4$  with  $\text{CO}_2$  corresponding to the different experimental conditions: A–E (see Table III for the details). These pictures have been made from the screen of the oscilloscope.

conditions for DBD, probably due to initial accumulation of the  $\text{C}_2$ -compounds in the gas phase and formation of the polymer film on the dielectric surface. After these initial alterations, the shape of the charge-voltage characteristics remained unchanging until the end of a measurement. The characteristics shown in Fig. 7 correspond to the final steady-state conditions.

Comparison of the Lissajous figures for the experimental conditions denoted as A and D (Table III, Fig. 7A and 7D) leads to the conclusion that the addition of He to the working gas mixture results in an increase of the transferred charge values for the negative polarity of the dielectric, and on the contrary, to a decrease of these quantities for the positive polarity. Very similar influence of He on the shapes of the charge-voltage characteristics was observed also in the

case of the binary mixtures of He with  $\text{CH}_4$ .<sup>(11)</sup> There are some slight but noticeable differences between the Lissajous figures corresponding to the new glass electrode (Fig. 7B), and to that after recovery (Fig. 7D). As we expected, using the ferroelectric ceramic as a dielectric electrode causes a considerable rise of the transferred charge values (Fig. 7E). It is interesting that almost the same effect is observed also in the case of strongly oxidized polymer film on the glass surface, however only for the positive polarity of the dielectric (Fig. 7C).

Although it seems to be hardly possible to give some simple explanation for the already-described dependence of the shapes of the charge-voltage characteristics of the DBD upon the state of the dielectric surface, the Lissajous figures technique has been proved to be a valuable tool to monitor the operating conditions of the discharge.

Chemical yields of eight typical reaction products (saturated, unsaturated hydrocarbons, oxygen-containing compounds) are shown in Fig. 8 for experimental arrangements A-E (Table III). Energetic yields of these reaction products are compared with the corresponding experimental results of Eliasson *et al.*<sup>(20)</sup> (set F in Fig. 8). Despite the already-mentioned great difference in experimental conditions, both sets of experimental data appear to correspond to comparable ranges of energetic yields.

Comparison of the data sets A and E with D (Fig. 8) leads to the following conclusions. The addition of He (expected to increase the effective value of

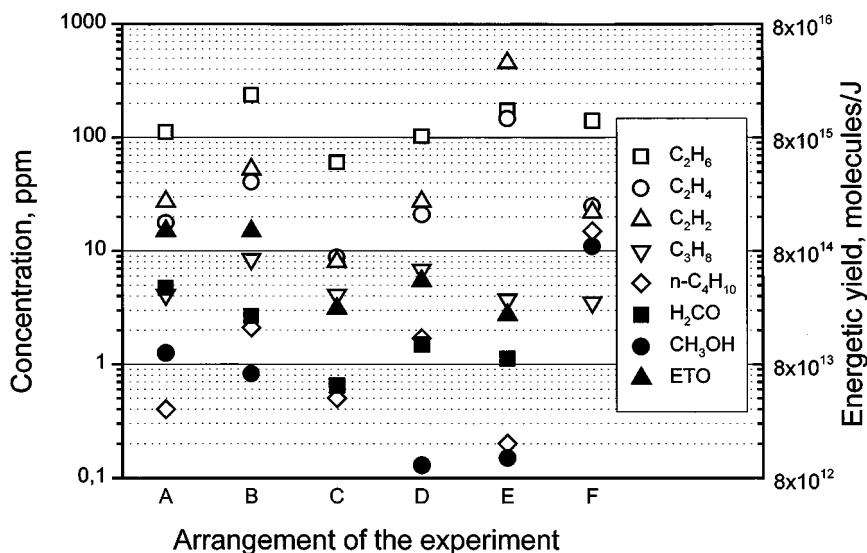


Fig. 8. Comparison of the chemical efficiencies of the DBD in the mixtures of  $\text{CH}_4$  with  $\text{CO}_2$  for the different experimental conditions: A-E (see Table III for the details). Set F—experimental results.<sup>(20)</sup>

mean electron energy) promotes the syntheses of oxygenated organic compounds ( $\text{H}_2\text{CO}$ ,  $\text{CH}_3\text{OH}$  and  $\text{ETO}$ ), and inhibits the formation of unsaturated hydrocarbons via the overall reactions (2) and (3). An increase of the power density due to the ceramic covering (data set E) causes considerable growth of the yields of unsaturated hydrocarbons ( $\text{C}_2\text{H}_2$  and  $\text{C}_2\text{H}_4$ ), but does not appear to benefit the production of alkanes and oxygenated organic compounds.

Thus, treating the described peculiarities of the dominant reaction pathway schemes for the experimental arrangements A and E as the consequences of the effects of increasing the mean electron energy (A), or electric power density (E), we can proceed to the comparative analysis of the data sets B, C and D, that differ from each other only by the state (quality) of the glass electrode surface. This analysis allows us to conclude that in the succession B - D - C (i.e., new glass - glass surface after recovery—strongly oxidized glass surface) the gradual drop of the concentrations of all the reaction products is caused by the decrease of the mean electron energy, rather than by the rise of electric power density, as it might be expected from the comparison of the corresponding charge-voltage characteristics (Fig. 8).

#### 4. GENERAL SCHEME OF REACTION PATHWAYS AND CONCLUSIONS

Almost all of the previously-considered plasma chemical products and overall reactions are schematically presented in Fig. 9. Three inorganic reaction products ( $\text{H}_2$ ,  $\text{H}_2\text{O}$ , and  $\text{CO}$ ) not monitored within the present experimental study, and the corresponding chemical pathways are denoted in Fig. 9 by the dashed lines and arrows.

In this scheme it is implied that in the system under consideration only  $\text{CH}_4$ ,  $\text{CO}_2$  and  $\text{C}_2$ -hydrocarbons (i.e., only the species not removed from the gas phase by the cold trap) are subjected to the treatment by the DBD-plasma. Actually, before being trapped, the other reaction products may be also decomposed, at least partly, by direct electron impact. For example, methanol has been demonstrated to be readily decomposed in the DBD.<sup>(23)</sup>

The mechanism of three sequential steps for the formation of  $\text{C}_2$  hydrocarbons (see Eq. (1), Fig. 9, and Refs. 16 and 18) implies the absence of the overall reactions  $\text{CH}_4 \rightarrow \text{C}_2\text{H}_4$  and  $\text{CH}_4 \rightarrow \text{C}_2\text{H}_2$ . However, the latter chemical pathways are often observed in another electrical discharges (for example, in a microwave afterglow plasma<sup>(19)</sup>). The corresponding kinetic schemes include reaction channels with the participation of the radicals  $\text{CH}_2$ ,  $\text{CH}$ ,  $\text{C}$ ,  $\text{C}_2\text{H}_3$  and  $\text{C}_2\text{H}$ , which formation seems to be highly improbable under the conditions of DBD (relatively low gas temperature and power density within the microdischarge channels<sup>(9,10)</sup>).

From these results, it follows that there are at least two possibilities to vary the contributions of different chemical pathways shown in the Fig. 9. First, using

Chemical conversions in the mixtures  $\text{CH}_4 + \text{CO}_2$  in the DBD

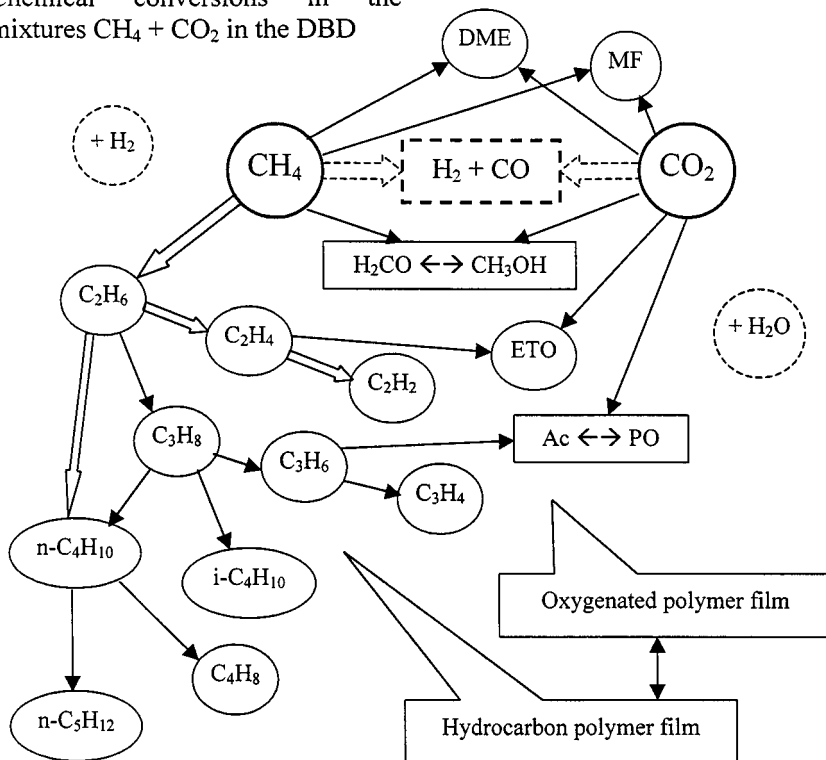


Fig. 9. An outline of the dominant chemical processes in the DBD in the mixtures  $\text{CH}_4 + \text{CO}_2$  at atmospheric pressure.

of an open gas flow system instead of a closed one may be expected to prevent multi-step processes from occurring, in particular polymer film formation (bottom part of the scheme in Fig. 9). Second, an increase in specific power density within the microdischarge channels appears to promote the de-hydrogenation processes (a shift from the left to the right in the central part of the scheme under consideration).

## ACKNOWLEDGMENT

The work was supported by the German Research Foundation within the Sonderforschungsbereich 198-Kinetics of partially ionized gases.

## REFERENCES

1. H. Buff and A. W. Hoffman, *J. Chem. Soc.* **12**, 282 (1860).
2. M. Berthelot, *C. R., Compt. Rend.* **82**, 1357 (1876).

3. M. Berthelot, *Ann. Chim. Phys.* **10**, 69 (1877).
4. J. R. Hollohan and A. T. Bell (eds.), *Techniques and Application of Plasma Chemistry*, John Wiley, New York (1974).
5. S. S. Shepelev, H. D. Gesser, and N. R. Hunter, *Plasma Chem. Plasma Process.* **13**, 479 (1993).
6. L. M. Zhou, B. Xue, U. Kogelschatz, and B. Eliasson, *Plasma Chem. Plasma Process.* **18**, 375 (1998).
7. S. P. Bugaev, V. A. Kuvshinov, N. S. Sochugov, and P. A. Khryapov, *Proc. Fifth Int'l. Symp. on High Pressure Low Temp. Plasma Chem. (HAKONE-5)*, Milovy, Czech Republic, 145 (1996).
8. U. Kogelschatz, B. Eliasson, and W. Egli, *Proc. 23rd Int'l. Conf. on Phenomena in Ionized Gases*, Toulouse, France, **1**, (1997): Invited papers C4-47 to C4-66.
9. B. Eliasson and U. Kogelschatz, *IEEE Trans. Plasma Sci.* **19**, 309 (1991).
10. V. Samoilovich, V. Gibalov, and K. Kozlov, *Physical Chemistry of the Barrier Discharge*, Second Edition Düsseldorf, DVS Verlag (1997).
11. K. V. Kozlov, P. Michel, and H.-E. Wagner, *Czech. J. Phys.* **48**, 1199 (1998).
12. K. V. Kozlov, P. Michel, and H.-E. Wagner, *Proc. 14th Int'l. Symp. on Plasma Chem., (ISPC-14)*, Prague, Czech Republic **4**, 1849 (1999).
13. K. V. Kozlov, P. Michel, and H.-E. Wagner, *Proc. Sixth Int'l. Symp. on High Pressure Low Temp. Plasma Chem. (HAKONE-5)*, Cork, Ireland, 78 (1998).
14. L. M. Zhou, B. Xue, U. Kogelschatz, and B. Eliasson, *Energy Fuels* **12**, 1191 (1998).
15. O. Montret, S. Pellerin, M. Nikravec, V. Massereau, and J. M. Pouvesle, *Plasma Chem. Plasma Process.* **17**, 393 (1997).
16. Yu. N. Zhitnev and Yu. V. Filippov, *Vestnik Moskovskogo Universiteta, Khimiya* **1**, 8 (1967).
17. E. Ruzinska, M. Kurdel, and M. Morvova, *Proc. Fifth Int'l. Symp. on High Pressure Low Temp. Plasma Chem. (HAKONE-5)*, Milovy, Czech Republic, 290 (1996).
18. R. V. St. Auney, *Chimie et Industrie* **29**, 1011 (1933).
19. J.-C. Legrand, A.-M. Diany, R. Hrach, and V. Hrachova, *Contrib. Plasma Phys.* **37**, 521 (1997).
20. B. Eliasson, U. Kogelschatz, E. Killer, and A. Bill, *Proc. 11th World Hydrogen Energy Conf.*, Stuttgart, Germany, **3**, 2449 (1996).
21. B. Eliasson, U. Kogelschatz, B. Xue, and L. M. Zhou, *Ind. Eng. Chem. Res.* **37**, 3350 (1998).
22. A. Sonnenfeld, T. M. Tun, and J. F. Behnke, *Proc. 14th Int'l. Symp. on Plasma Chem., (ISPC-14)* Prague, Czech Republic, **3**, 1315 (1999).
23. A. Szymanski and T. Opalinska, *Acta Physica Slovaca* **35**, 363 (1985).